POLITECNICO DI TORINO
Repository ISTITUZIONALE

Topological Quantum Critical Points in the Extended Bose-Hubbard Model

Original
Topological Quantum Critical Points in the Extended Bose-Hubbard Model / Fraxanet, J., Gonzalez-Cuadra, D., Pfau, T., Lewenstein, M., Langen, T., Barbiero, L.. - In: PHYSICAL REVIEW LETTERS. - ISSN 0031-9007. - ELETTRONICO. - 128:4(2022), p. 043402. [10.1103/PhysRevLett.128.043402]

Availability:
This version is available at: 11583/2959123 since: 2022-03-22T12:04:06Z

Publisher:
American Physical Society

Published
DOI:10.1103/PhysRevLett.128.043402

Terms of use:

This article is made available under terms and conditions as specified in the corresponding bibliographic description in the repository

Publisher copyright

(Article begins on next page)

27 November 2026

Topological Quantum Critical Points in the Extended Bose-Hubbard Model

Joana Fraxanet,[1,*] Daniel González-Cuadra,[1,2,3] Tilman Pfau,[4] Maciej Lewenstein,[1,5] Tim Langen,[4] and Luca Barbiero[1,6,†]

[1]*ICFO—Institut de Ciències Fotòniques, The Barcelona Institute of Science and Technology, 08860 Castelldefels, Barcelona, Spain*
[2]*Center for Quantum Physics, University of Innsbruck, 6020 Innsbruck, Austria*
[3]*Institute for Quantum Optics and Quantum Information of the Austrian Academy of Sciences, 6020 Innsbruck, Austria*
[4]*5. Physikalisches Institut and Center for Integrated Quantum Science and Technology, Universität Stuttgart, Pfaffenwaldring 57, 70569 Stuttgart, Germany*
[5]*ICREA, Passeig Lluis Companys 23, ES-08010 Barcelona, Spain*
[6]*Institute for Condensed Matter Physics and Complex Systems, DISAT, Politecnico di Torino, I-10129 Torino, Italy*

(Received 6 July 2021; accepted 3 January 2022; published 27 January 2022)

The combination of topology and quantum criticality can give rise to an exotic mix of counterintuitive effects. Here, we show that unexpected topological properties take place in a paradigmatic strongly correlated Hamiltonian: the 1D extended Bose-Hubbard model. In particular, we reveal the presence of two distinct topological quantum critical points with localized edge states and gapless bulk excitations. Our results show that the topological critical points separate two phases, one topologically protected and the other topologically trivial, both characterized by a long-range ordered string correlation function. The long-range order persists also at the topological critical points and explains the presence of localized edge states protected by a finite charge gap. Finally, we introduce a superresolution quantum gas microscopy scheme for dipolar dysprosium atoms, which provides a reliable route towards the experimental study of topological quantum critical points.

DOI: 10.1103/PhysRevLett.128.043402

Introduction.—Topology represents a fascinating topic in different areas of modern quantum physics [1–3]. Among the related interesting phenomena one finds conducting edge modes in bulk gapped phases [4,5], quantized conductance [6–9], and fractionalized charges [10–12]. Because of the gapped and nonlocal nature of their elementary excitations, topological phases further represent a particularly suitable platform where fault-tolerant quantum computation could be performed [13–17].

While in noninteracting systems [18] symmetry arguments allow for a complete description of topological insulators [19–21] and superconductors [22], topology in many-body quantum systems represents a more challenging task [23]. In this context, the notion of symmetry-protected topological (SPT) phases [24–27] has allowed us to classify quantum states that are topologically protected up to local perturbations preserving specific symmetries. Celebrated examples of such fully gapped topological states include the Haldane phase occurring in several strongly correlated systems [28–45], and the topological Mott insulator (TMI) appearing in interacting Su-Schrieffer-Heger (SSH) models [46–54]. Noticeably, the impressive the level of flexibility and accuracy reachable in ultracold atomic platforms has allowed for the experimental realizations of these SPT phases [55,56].

Recent works have further shown that, contrary to standard intuition, topology can also occur in critical phases [27,57–71]. Here, topological phase transitions deserve special attention. As shown in specific models [67], topologically protected edge states (ESs) can remain localized at critical points despite the presence of gapless bulk excitations. Because of the novelty of such a concept, the mechanism that topologically protects quantum critical points is not yet fully understood.

The results reported in this Letter provide grounds for a better comprehension of topological quantum critical points (TQCPs). Our analysis, based on density-matrix renormalization-group (DMRG) [72–74] calculations, shows that these states of matter occur in distinct regimes of the broadly investigated 1D extended Bose-Hubbard model (EBHM). Here, we unveil that, for large enough interaction, different TQCPs take place both at unit density and at half filling in the presence of a lattice dimerization. Despite the usual vanishing bulk gap at quantum criticality, our results show that topology remains protected by a finite charge gap. This scenario holds in quantum critical points separating a topological and a trivial phase, both sharing a similar type of long-range order captured by the same string correlation function. This hypothesis is confirmed by studying other topological phase transitions between phases without such order, where the charge gap vanishes and the topological properties disappear.

We further present a reliable route to probe the existence of TQCPs through a quantum-simulation scheme involving

 © 2022 American Physical Society

magnetic atoms with dipolar long-range interaction [75]. The latter have been recently employed to study droplets physics [76,77], thermalization [78], supersolidity [79–81], topological pumping [82], and notably, to simulate the EBHM [83]. However, the dipolar interaction in current experimental setups has been too weak to explore the full EBHM phase diagram. We propose a new quantum gas microscopy scheme based on strongly interacting dysprosium atoms trapped in a short wavelength optical lattice, which allows us to make precise predictions about the experimental realization and detection of TQCPs.

Model.—The 1D EBHM reads as

$$H = -\sum_{i=1}^{L-1}(J+\delta J(-1)^i)(b_i^\dagger b_{i+1} + \text{H.c.}) + \frac{U}{2}\sum_{i=1}^{L} n_i(n_i-1) + V\sum_{i=1}^{L-1} n_i n_{i+1}, \quad (1)$$

where $b_i^\dagger(b_i)$ is the bosonic operator describing the creation (annihilation) of a particle at the i-site of a lattice of length L filled with N bosons. The tunneling amplitude $J-\delta J$ ($J+\delta J$) describes hopping processes in odd (even) links connecting two nearest-neighbor (NN) sites while U and V represent, respectively, the on-site and NN interactions. The most investigated version of Eq. (1) is the homogeneous case $\delta J = 0$ at unit density $\bar{n} = N/L = 1$. Here, early studies [84,85] discovered the presence of a gapless superfluid in the limit of weak interaction, a Mott insulator (MI) in the regime of strong on-site repulsion and, for large enough V, a charge density wave (CDW_1). The CDW_1 is characterized by a staggered density pattern of alternated pairs and empty sites, analogous to the effective antiferromagnetic (AFM) order of the XXZ spin-1 chain which, for large U/J, represents an accurate description of the EBHM [30,34,40]. This analogy has induced the discovery of a fully gapped SPT phase with nonlocal AFM order between pairs and empty sites occurring at intermediate couplings strength [30]. The latter corresponds to the celebrated Haldane insulator (HI), which in the EBHM is protected by effective spin rotational symmetries and exact inversion symmetry [86]. Instead, the dimerized case, $\delta J > 0$, has been only partially investigated [87,88]. At $\bar{n} = 1/2$, the large U/J regime unveils the presence of a phase transition between an inversion symmetry protected topological Mott insulator (TMI) and a trivial charge density wave ($\text{CDW}_{1/2}$) with local AFM order signaled by a staggered density pattern of alternated empty and single occupied sites [89]. Although the gapped topological phases in Eq. (1) are understood, the study of possible topological states appearing at quantum critical points remains an open challenge.

Homogeneous case ($\delta J = 0$) at $\bar{n} = 1$.—SPT phases are characterized by two main features: degenerate localized ESs and gapped bulk excitations. The first requirement is tested by examining the edge localization length ξ_e, which, for a phase hosting ESs, is extracted from $|E_+ - E_-| \sim e^{-L/\xi_e}$. Here, $E_\pm$ are the energies of the two degenerate ground states, $|L\rangle \pm |R\rangle$, where $|L\rangle(|R\rangle)$ denotes a state with the left (right) ES occupied by a bosonic pair and the right (left) ES empty [90]. In particular, a thermodynamic extrapolation is expected to show $\xi_e^{-1} \neq 0$ in the presence of localized ESs and $\xi_e^{-1} \to 0$ as they delocalize and become bulk states. Analogously, gapped bulk excitations are captured by a finite value of the bulk correlation length $\xi_b \sim \Delta E_{\text{bulk}}^{-1}$, where $\Delta E_{\text{bulk}} = E_1 - E_{\text{GS}}$ is the lowest energy bulk gap and E_{GS} (E_1) is the energy of the ground (first excited) state. As usual, at quantum criticality $\Delta E_{\text{bulk}} = 0$ and therefore ξ_b diverges. In Figs. 1(a)–1(b), our calculations show that the HI has all the aforementioned features, namely, $\xi_e^{-1}, \xi_b^{-1} \neq 0$. Probing the SPT nature of HI demands uniquely nonlocal order parameters. More specifically, the parameters describing the HI are $\mathcal{O}_{1,\alpha}(j) = e^{\imath\pi\sum_{k<j} S_1^\alpha(k)} S_1^\alpha(j)$, with $\alpha = x, z$, $S_1^x(i) = (1/\sqrt{2})[\sqrt{1-(n_i/2)}b_i + b_i^\dagger\sqrt{1-(n_i/2)}]$, and

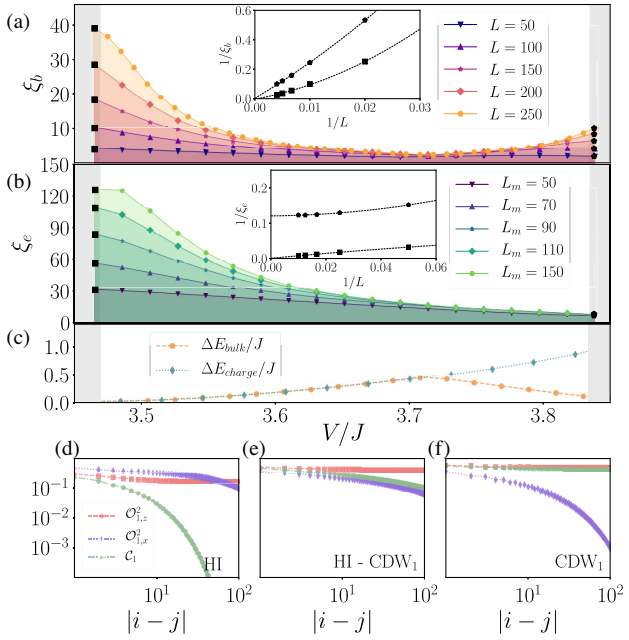


FIG. 1. DMRG calculations of edge ξ_e (a) and bulk ξ_b (b) correlation length in units of the lattice spacing a_{lat}, with parameters $\bar{n} = 1$, $\delta J = 0$, $U/J = 6$ as a function of V/J. The insets show the finite size extrapolation of ξ_e and ξ_b at the MI-HI (squares) and HI-CDW_1 (pentagons) critical points. L_m is the maximum length to extract ξ_e from a linear fit of $\log(|E_+ - E_-|)$ versus L [106]. (c) Bulk gap ΔE_{bulk} (orange) and charge gap ΔE_{charge} (blue) for $L = 200$. The gaps are computed by fixing the edge occupation by means of large chemical potential. iDMRG calculations of the decay of $\mathcal{C}_1$ (green), $\mathcal{O}^2_{1,x}$ (purple), and $\mathcal{O}^2_{1,z}$ (magenta) relative to: HI at $V/J = 3.65$ (d), the HI-CDW_1 critical point at $V/J = 3.86$, (e) and CDW_1 at $V/J = 3.91$ (f). We employ a bond dimension $D = 250$ and we cut the number of bosons per site at $n_0 = 4$.

$S^z_1(i) = 1 - n_i$ [34]. The HI is therefore characterized by the long-range order [91,92] of the string correlators

$$\mathcal{O}^2_{1,\alpha}(|i-j|) = \langle \mathcal{O}_{1,\alpha}(i)\mathcal{O}_{1,\alpha}(j)\rangle, \qquad \alpha = x, z. \quad (2)$$

Because of the breaking of the effective rotational $x \leftrightarrow z$ symmetry, the two strings $\mathcal{O}^2_{1,\alpha}$ are expected to behave differently in CDW_1. In particular, the local AFM order of CDW_1 is characterized by an exponential decay of $\mathcal{O}^2_{1,x}$ but preserved long-range order of $\mathcal{O}^2_{1,z}$. Crucially, the CDW_1 has no topological features since, as discussed, its local magnetic order is captured by the two points correlator

$$\mathcal{C}_1(|i-j|) = \langle S^z_1(i) S^z_1(j)\rangle. \quad (3)$$

In Figs. 1(d) and 1(f) we obtain the expected behavior of Eqs. (2) and (3) in the HI and the CDW_1. By varying V/J at intermediate values of U/J, a Gaussian and an Ising phase transition describing, respectively, the MI-HI and HI-CDW_1 critical points are found [93]. As expected, and confirmed by the diverging ξ_b shown in Fig. 1(a), the bulk gap vanishes at the transition points, see Fig. 1(c). The absence of a bulk gap may suggest that localized ESs also disappear. On the contrary, our calculations demonstrate that this is not always the case. In particular, while at the Gaussian phase transition ξ_b^{-1}, $\xi_e^{-1} = 0$, at the HI-CDW_1 critical point the edge localization length ξ_e remains finite in the thermodynamic limit. This proves the presence of localized ESs formed by an empty site and a pair of bosons. Moreover, as reported in Fig. 1(e), this critical point shows algebraic decay of both $\mathcal{O}^2_{1,x}$ and $\mathcal{C}_1$, while $\mathcal{O}^2_{1,z}$ preserves the long-range order. As discussed, the algebraic decay of $\mathcal{C}_1$ does not occur in the HI, thus implying that a different topological phase exists at this critical point.

In order to understand the origin of such TQCP, we show in Fig. 1(c) how a gap at energies higher than ΔE_{bulk}, i.e., the charge gap $\Delta E_{\mathrm{charge}} = E_{\mathrm{GS}}(N+1, L) + E_{\mathrm{GS}}(N-1, L) - 2E_{\mathrm{GS}}(N, L)$ associated to the AFM ordering in both HI and CDW_1, does not vanish at the HI-CDW_1 transition point. This explains why at this TQCP, see Fig. 1(e), we still find long-range order of uniquely a string correlator, namely, $\mathcal{O}^2_{1,z}$, as required in SPT phases. As a consequence, it is natural to state that the $\Delta E_{\mathrm{charge}}$ is the responsible for the protection of the ESs. It is worth to underline that this analysis can be used to interpret the physics of spin-1 chains where the same TQCP takes place [67]. In the latter case, a finite $\Delta E_{\mathrm{charge}}$ corresponds to a finite spin gap [40] and the string order parameter along the z axis is still expected to be finite at criticality, see the Supplemental Material [93]. As known [30,31,40,107], for $U = 0$ and truncated local Hilbert space to $n_0 = 2$, the homogeneous case is strictly equivalent to a spin-1 XXZ chain [108]. Interestingly, our results fully characterize a TQCP away from this spin-1 limit, thus generalizing the physics of TCPQs to new regimes of the EBHM. We show that for relatively large U/J, inversion symmetry combined with effective rotational symmetries are still able to give rise to TQCPs. We now explore whether similar TQCPs appear when effective spin-1 representations are not applicable.

Dimerized case ($\delta J > 0$) at $\bar{n} = 1/2$.—In this regime, a TMI appears for large enough U/J and intermediate or vanishing V/J [87,88]. Notice that such phase displays features analogous to the SPT phase appearing in the dimerized spin-1/2 Heisenberg model [109]. The topology of TMI is protected by the inversion symmetry and, although the bulk-edge correspondence does not hold due to the absence of chiral symmetry, localized ESs appear for large enough values of U/J [87], see Fig. 2(b). In this case, the ESs are given by either a vanishing or single occupation. Figure 2(a) shows a finite bulk correlation length in the TMI phase, and in Fig. 2(d) we report that the topological nature of TMI is effectively captured by the long-range order of specific nonlocal string correlators

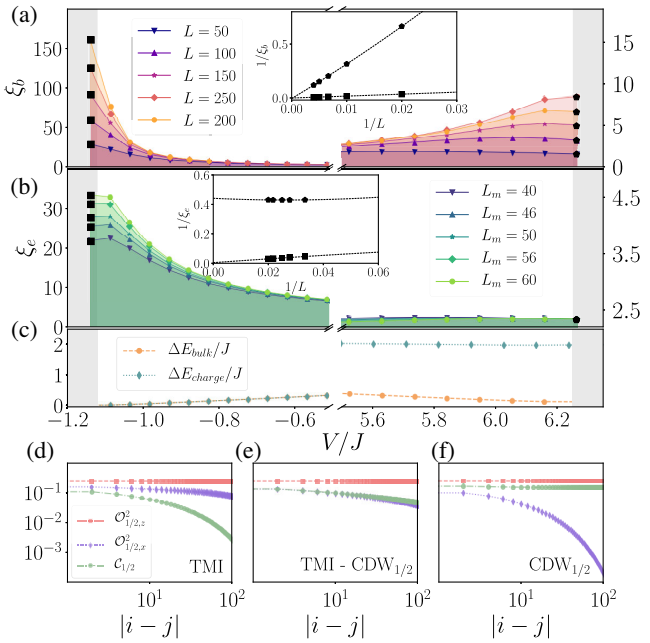


FIG. 2. DMRG calculations of the edge ξ_e (a) and bulk ξ_b (b) correlation length in units of the lattice spacing a_{lat}, with parameters $\bar{n} = 1/2$, $\delta J = 0.5$, $U/J = 6$ as a function of V/J. The insets show the finite size extrapolation of ξ_e and ξ_b at the PS-TMI (squares) and TMI-$\mathrm{CDW}_{1/2}$ (pentagons) critical points. L_m is the maximum length to extract ξ_e from a linear fit of $\log(E_+ - E_-)$ versus L [106]. (c) Bulk gap ΔE_{bulk} (orange) and charge gap $\Delta E_{\mathrm{charge}}$ (blue) for $L = 200$. The gaps are computed by fixing the edge occupation by means of large chemical potential. iDMRG calculations of the decay of $\mathcal{C}_{1/2}$ (green), $\mathcal{O}^2_{1/2,x}$ (purple), and $\mathcal{O}^2_{1/2,z}$ (magenta) relative to TMI at $V/J = 6.03$ (d), the TMI-$\mathrm{CDW}_{1/2}$ critical point at $V/J = 6.35$ (e), and $\mathrm{CDW}_{1/2}$ at $V/J = 6.97$ (f). We employ a bond dimension $D = 250$ and we cut the number of bosons per site at $n_0 = 3$.

$$\mathcal{O}^2_{1/2,\alpha}(|i-j|) = \langle \mathcal{O}_{1/2,\alpha}(2i-1)\mathcal{O}_{1/2,\alpha}(2j)\rangle, \qquad \alpha = x, z. \tag{4}$$

signaling nonlocal magnetic order between odd and even sites with alternated bosonic occupation. Here, the associated nonlocal order parameters are $\mathcal{O}_{1/2,\alpha}(j) = e^{\imath\pi\sum_{k<j} S^{\alpha}_{1/2}(k)} S^{\alpha}_{1/2}(j)$ with $S^z_{1/2}(i) = (1/2 - n_i)$ and $S^x_{1/2}(i) = 1/2(\sqrt{1-n_i}b_i + b_i^{\dagger}\sqrt{1-n_i})$. For $V < 0$, a diverging compressibility signals the presence of a first order phase transition to a regime of phase separation [93]. At the transition point we find that ξ_e^{-1}, $\xi_b^{-1} = 0$, meaning that the ESs disappear and the topology is destroyed. Instead, for larger V/J the system undergoes a phase transition where the TMI is replaced by a trivial $\mathrm{CDW}_{1/2}$, captured by the long-range order of the two points correlator

$$\mathcal{C}_{1/2}(|i-j|) = \langle S^z_{1/2}(i) S^z_{1/2}(j)\rangle. \tag{5}$$

As in the previous case, the TMI and $\mathrm{CDW}_{1/2}$ have, respectively, nonlocal and local AFM order which now reflects the alternation between empty and singly occupied sites. In Fig. 2(a) we report that the critical point connecting the $\mathrm{CDW}_{1/2}$ and TMI is, as expected, signaled by $\xi_b^{-1} = 0$, which follows from $\Delta E_{\mathrm{bulk}} = 0$, see Fig. 2(c). Crucially, in Fig. 2(b) we reveal that localized ESs captured by a finite ξ_e remain stable at this transition point. The topological ESs are formed by an empty and single occupied state, thus different from the TQCP observed for $\delta J = 0$. Moreover, this TQCP is further characterized by an algebraic decay of $\mathcal{O}^2_{1/2,x}$ and $\mathcal{C}_{1/2}$ [Fig. 2(e)]. In this case, the TQCP is protected uniquely by inversion symmetry, but as shown in Ref. [93], the same results are found for the hardcore limit, where the topological ESs are formally protected by the combination of inversion symmetry and chiral symmetry. Furthermore, as we show Fig. 2(c), the topological ESs in the TQCP and the long-range order of the z-oriented string correlator $\mathcal{O}^2_{1/2,z}$, which effectively captures the topological nature of the critical point, are again protected by a nonvanishing charge gap.

The results on the dimerized case provide a new example of a TQCP substantially different from the one found for $\delta J = 0$. More importantly, they also confirm the hypothesis that the two studied cases share a common mechanism as the one responsible for the appearance of TQCPs. Our results point in the direction that if two gapped phases, one topologically protected and the other trivial, are both characterized by a similar long-range order captured by a string correlator, as a consequence, the two phases are connected by a TQCP.

Experimental realization and detection of a TQCP.—In this section we discuss how to observe TQCPs using ultracold dysprosium atoms in an optical lattice. In addition to the usual contact interactions, the large magnetic dipole moment of $10\mu_B$, where μ_B denotes the Bohr magneton, makes such atoms interact highly nonlocally through dipole-dipole repulsion. Since such interaction scales as $1/r^3$, it is necessary to trap the atoms in a lattice with short periodicity in order to achieve sizable NN interactions. A lattice formed using lasers with a wavelength around 360 nm is promising for this purpose [93]. The corresponding lattice spacing $a_{\mathrm{lat}} = 180$ nm results in a NN interaction strength of $V/h \sim 200$ Hz, where h is Planck's constant. This is an enhancement by a factor of six compared to previous experiments with magnetic atoms [83] and a factor of four compared to dipolar molecules [110]. As shown in Fig. 3, and explained in detail in the Supplemental Material [93], by changing the lattice depth V_0/E_R and tuning the on-site interaction between atoms using a Feshbach resonance [111,112], it is possible to achieve values of interactions where TQCPs can be explored. Notice that in one dimension and for not too large V, dipolar interaction can neither produce new phases with respect to NN interactions nor change the nature of the transition points. For this reason, our cut of the dipolar interaction to NN is a reliable approximation. Moreover, strongly coupled bilayer geometries could be realized by implementing a subwavelength optical barrier inside the individual lattice sites of a 1D lattice [113]. In this way, an effective dimerization $\delta J > 0$ can be achieved. Thanks to the strong dipolar interaction, we also estimate a critical temperature required to stabilize the topological phase on the order of tens of nK, well within the reach of current experiments. In such a setting, two-point density-density correlation functions $\mathcal{C}_1$ and $\mathcal{C}_{1/2}$, string correlators $\mathcal{O}^2_{1,z}$ and $\mathcal{O}^2_{1/2,z}$, and edge correlation lengths ξ_e are directly

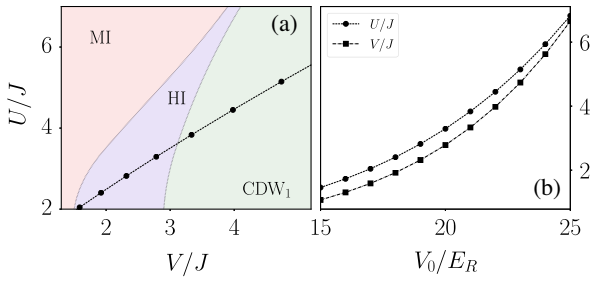


FIG. 3. (a) Qualitative phase diagram of Eq. (1) at $\delta J = 0$ and $\bar{n} = 1$ [36]. The circles represent examples of experimentally accessible values of U/J and V/J calculated by considering dysprosium atoms with dipole moment of $10\mu_B$ and s-wave scattering length $a_{3\mathrm{D}} = 91a_0$ with a_0 the Bohr radius. The atoms are trapped in a lattice with longitudinal lattice spacing $a_{lat} = 180$ nm and transverse confinement of frequency $\omega_{\perp} = 2\pi \times 4$ kHz, see Ref. [93] for details. (b) Values of U/J (circles) and V/J (squares) calculated by considering lattice depth V_0/E_R ranging from 15 to 25. Notice that different choices of $a_{3\mathrm{D}}$ and $\omega_{\perp}$ allow us to achieve different sectors of the phase diagram.

accessible using quantum gas microscopy [55,114,115]. However, the requirement of a short lattice wavelength poses a significant challenge for quantum gas microscopy, as the lattice wavelength is significantly below the Abbe resolution limit for the 421 nm imaging transition in dysprosium. As we show in Ref. [93], this limitation can be overcome by using superresolution techniques to detect individual atoms below the diffraction limit. This scheme results to be inherently number resolving and can allow to individually image empty sites, as well as higher-order occupations, thus allowing for a complete characterization of TQCPs.

Discussion and outlook.—We have shown that the recently discovered phenomenon of topological phases occurring at quantum critical points can be explored in the celebrated EBHM. The TQCPs are SPT phases with gapless bulk excitations but, at the same time, localized edge states. Our analysis has revealed how different kinds of TQCPs are found by adjusting the Hamiltonian parameters. Furthermore, we revealed that TQCPs take place between two fully gapped phases, one topological and one trivial, when they are both characterized by a finite value of the same string correlator denoting a similar type of long-range order. In this scenario, we have demonstrated that, at criticality, a finite charge gap is able to protects the localized edge states. In order to provide a reliable route towards the experimental investigation of TQCPs, we have proposed a detailed experimental setup involving trapped dysprosium atoms at ultracold temperatures. Here, on one hand, laser beams producing short lattice spacing can be employed to achieve the desired region of the phase diagram and, on the other hand, a quantum gas microscope with superresolution techniques can allow for an accurate detection of TQCPs. Because of the fact that EBHMs are of great relevance in different physical systems [116–120], we expect that our results can stimulate the study of TQCPs in a broad variety of research lines.

We thank A. Dauphin, A. Montorsi, G. Palumbo, F. Pollmann, and R.Verresen for discussion. J. F., D. G-C., M. L., and L. B. acknowledge support from ERC AdG NOQIA, Spanish Ministry MINECO, and State Research Agency AEI (Severo Ochoa Center of Excellence CEX2019-000910-S, Plan National FIDEUA PID2019-106901GB-I00/10.13039/501100011033, FPI), Fundació Cellex, Fundació Mir-Puig, Generalitat de Catalunya (AGAUR Grant No. 2017 SGR 1341, CERCA program, QuantumCAT U16-011424, co-funded by ERDF Operational Program of Catalonia 2014–2020), EU Horizon 2020 FET-OPEN OPTOLogic (Grant No. 899794) and the National Science Centre, Poland (Symfonia Grant No. 2016/20/W/ST4/00314), Marie Skłodowska-Curie grant STREDCH No. 101029393, La Caixa Junior Leaders fellowships (ID100010434), and EU Horizon 2020 under Marie Skłodowska-Curie Grant Agreement No. 847648 (LCF/BQ/PI19/11690013, LCF/BQ/PI20/11760031, LCF/BQ/PR20/11770012). D. G.-C. is supported by the Simons Collaboration on Ultra-Quantum Matter, which is a grant from the Simons Foundation (651440, P. Z.). T. L. acknowledges support from the Vector Stiftung and the European Research Council (ERC) under the European Union's Horizon 2020 research and innovation programme (Grant Agreement No. 949431). T. P. and T. L. acknowledge support by the German Research Foundation (DFG) within FOR2247 under Pf381/16-1 and Bu2247/1, Pf381/20-1, FUGG INST41/1056-1. We acknowledge QUANT:ERA collaborative project MAQS for financial support.

*joana.fraxanet@icfo.eu
†luca.barbiero@polito.it

[1] M. Asorey, Nat. Phys. **12**, 616 (2016).
[2] N. Goldman, J. C. Budich, and P. Zoller, Nat. Phys. **12**, 639 (2016).
[3] T. Ozawa, H. M. Price, A. Amo, N. Goldman, M. Hafezi, L. Lu, M. C. Rechtsman, D. Schuster, J. Simon, O. Zilberberg, and I. Carusotto, Rev. Mod. Phys. **91**, 015006 (2019).
[4] X.-L. Qi and S.-C. Zhang, Rev. Mod. Phys. **83**, 1057 (2011).
[5] M. Z. Hasan and C. L. Kane, Rev. Mod. Phys. **82**, 3045 (2010).
[6] K. v. Klitzing, G. Dorda, and M. Pepper, Phys. Rev. Lett. **45**, 494 (1980).
[7] R. B. Laughlin, Phys. Rev. B **23**, 5632 (1981).
[8] D. J. Thouless, M. Kohmoto, M. P. Nightingale, and M. denNijs, Phys. Rev. Lett. **49**, 405 (1982).
[9] N. Read and G. Moore, Prog. Theor. Phys. Suppl. **107**, 157 (1992).
[10] D. C. Tsui, H. L. Stormer, and A. C. Gossard, Phys. Rev. Lett. **48**, 1559 (1982).
[11] R. B. Laughlin, Phys. Rev. Lett. **50**, 1395 (1983).
[12] W. P. Su and J. R. Schrieffer, Phys. Rev. Lett. **46**, 738 (1981).
[13] A. Kitaev, Ann. Phys. (Amsterdam) **303**, 2 (2003).
[14] M. H. Freedman, Proc. Natl. Acad. Sci. U.S.A. **95**, 98 (1998).
[15] S. B. Bravyi and A. Y. Kitaev, arXiv:quant-ph/9811052.
[16] M. H. Freedman and D. A. Meyer, Found. Comput. Math. **1**, 325 (2001).
[17] E. Dennis, A. Kitaev, A. Landahl, and J. Preskill, J. Math. Phys. (N.Y.) **43**, 4452 (2002).
[18] A. Altland and M. R. Zirnbauer, Phys. Rev. B **55**, 1142 (1997).
[19] C. L. Kane and E. J. Mele, Phys. Rev. Lett. **95**, 146802 (2005).
[20] B. A. Bernevig and S.-C. Zhang, Phys. Rev. Lett. **96**, 106802 (2006).
[21] B. A. Bernevig, T. L. Hughes, and S.-C. Zhang, Science **314**, 1757 (2006).
[22] A. P. Schnyder, S. Ryu, A. Furusaki, and A. W. W. Ludwig, Phys. Rev. B **78**, 195125 (2008).
[23] L. Fidkowski and A. Kitaev, Phys. Rev. B **83**, 075103 (2011).

[24] F. Pollmann, A. M. Turner, E. Berg, and M. Oshikawa, Phys. Rev. B **81**, 064439 (2010).
[25] Z.-C. Gu and X.-G. Wen, Phys. Rev. B **80**, 155131 (2009).
[26] X. Chen, Z.-C. Gu, Z.-X. Liu, and X.-G. Wen, Science **338**, 1604 (2012).
[27] A. Montorsi, F. Dolcini, R. C. Iotti, and F. Rossi, Phys. Rev. B **95**, 245108 (2017).
[28] F. D. M. Haldane, Phys. Rev. Lett. **50**, 1153 (1983).
[29] I. Affleck, T. Kennedy, E. H. Lieb, and H. Tasaki, Phys. Rev. Lett. **59**, 799 (1987).
[30] E. G. Dalla Torre, E. Berg, and E. Altman, Phys. Rev. Lett. **97**, 260401 (2006).
[31] E. Berg, E. G. Dalla Torre, T. Giamarchi, and E. Altman, Phys. Rev. B **77**, 245119 (2008).
[32] H. Nonne, P. Lecheminant, S. Capponi, G. Roux, and E. Boulat, Phys. Rev. B **81**, 020408(R) (2010).
[33] M. Dalmonte, M. Di Dio, L. Barbiero, and F. Ortolani, Phys. Rev. B **83**, 155110 (2011).
[34] X. Deng and L. Santos, Phys. Rev. B **84**, 085138 (2011).
[35] S. Furukawa, M. Sato, S. Onoda, and A. Furusaki, Phys. Rev. B **86**, 094417 (2012).
[36] D. Rossini and R. Fazio, New J. Phys. **14**, 065012 (2012).
[37] K. Kobayashi, M. Okumura, Y. Ota, S. Yamada, and M. Machida, Phys. Rev. Lett. **109**, 235302 (2012).
[38] E. G. D. Torre, J. Phys. B **46**, 085303 (2013).
[39] L. Barbiero, A. Montorsi, and M. Roncaglia, Phys. Rev. B **88**, 035109 (2013).
[40] S. Ejima and H. Fehske, Phys. Rev. B **91**, 045121 (2015).
[41] S. Fazzini, A. Montorsi, M. Roncaglia, and L. Barbiero, New J. Phys. **19**, 123008 (2017).
[42] L. Barbiero, L. Dell'Anna, A. Trombettoni, and V. E. Korepin, Phys. Rev. B **96**, 180404(R) (2017).
[43] K. Kottmann, P. Huembeli, M. Lewenstein, and A. Acín, Phys. Rev. Lett. **125**, 170603 (2020).
[44] B. Hetényi, Phys. Rev. Research **2**, 023277 (2020).
[45] K. Kottmann, A. Haller, A. Acín, G. E. Astrakharchik, and M. Lewenstein, Phys. Rev. B **104**, 174514 (2021).
[46] S. R. Manmana, A. M. Essin, R. M. Noack, and V. Gurarie, Phys. Rev. B **86**, 205119 (2012).
[47] J. Sirker, M. Maiti, N. P. Konstantinidis, and N. Sedlmayr, J. Stat. Mech. (2014) P10032.
[48] D. Wang, S. Xu, Y. Wang, and C. Wu, Phys. Rev. B **91**, 115118 (2015).
[49] L. Barbiero, L. Santos, and N. Goldman, Phys. Rev. B **97**, 201115(R) (2018).
[50] B. Sbierski and C. Karrasch, Phys. Rev. B **98**, 165101 (2018).
[51] D. González-Cuadra, A. Dauphin, P. R. Grzybowski, P. Wójcik, M. Lewenstein, and A. Bermudez, Phys. Rev. B **99**, 045139 (2019).
[52] D. González-Cuadra, A. Bermudez, P. R. Grzybowski, M. Lewenstein, and A. Dauphin, Nat. Commun. **10**, 2694 (2019).
[53] X.-L. Yu, L. Jiang, Y.-M. Quan, T. Wu, Y. Chen, L.-J. Zou, and J. Wu, Phys. Rev. B **101**, 045422 (2020).
[54] T. Chanda, R. Kraus, G. Morigi, and J. Zakrzewski, Quantum **5**, 501 (2021).
[55] P. Sompet, S. Hirthe, D. Bourgund, T. Chalopin, J. Bibo, J. Koepsell, P. Bojovic, R. Verresen, F. Pollmann, G. Salomon, C. Gross, T. A. Hilker, and I. Bloch, arXiv: 2103.10421.
[56] S. de Léséleuc, V. Lienhard, P. Scholl, D. Barredo, S. Weber, N. Lang, H. P. Büchler, T. Lahaye, and A. Browaeys, Science **365**, 775 (2019).
[57] J. P. Kestner, B. Wang, J. D. Sau, and S. Das Sarma, Phys. Rev. B **83**, 174409 (2011).
[58] L. Fidkowski, R. M. Lutchyn, C. Nayak, and M. P. A. Fisher, Phys. Rev. B **84**, 195436 (2011).
[59] J. D. Sau, B. I. Halperin, K. Flensberg, and S. Das Sarma, Phys. Rev. B **84**, 144509 (2011).
[60] M. Cheng and H.-H. Tu, Phys. Rev. B **84**, 094503 (2011).
[61] A. Keselman and E. Berg, Phys. Rev. B **91**, 235309 (2015).
[62] T. Scaffidi, D. E. Parker, and R. Vasseur, Phys. Rev. X **7**, 041048 (2017).
[63] J. Ruhman and E. Altman, Phys. Rev. B **96**, 085133 (2017).
[64] D. E. Parker, T. Scaffidi, and R. Vasseur, Phys. Rev. B **97**, 165114 (2018).
[65] R.-X. Zhang and C.-X. Liu, Phys. Rev. Lett. **120**, 156802 (2018).
[66] R. Verresen, N. G. Jones, and F. Pollmann, Phys. Rev. Lett. **120**, 057001 (2018).
[67] R. Verresen, R. Thorngren, N. G. Jones, and F. Pollmann, Phys. Rev. X **11**, 041059 (2021).
[68] S. Fazzini, L. Barbiero, and A. Montorsi, Phys. Rev. Lett. **122**, 106402 (2019).
[69] A. Montorsi, S. Fazzini, and L. Barbiero, Phys. Rev. A **101**, 043618 (2020).
[70] T. Rakovszky, P. Sala, R. Verresen, M. Knap, and F. Pollmann, Phys. Rev. B **101**, 125126 (2020).
[71] R. R. Kumar, Y. R. Kartik, S. Rahul, and S. Sarkar, Sci. Rep. **11**, 1004 (2021).
[72] S. R. White, Phys. Rev. Lett. **69**, 2863 (1992).
[73] U. Schollwck, Ann. Phys. (Amsterdam) **326**, 96 (2011).
[74] J. Hauschild and F. Pollmann, SciPost Phys. Lect. Notes 5 (2018), code available from https://github.com/tenpy/tenpy.
[75] T. Lahaye, C. Menotti, L. Santos, M. Lewenstein, and T. Pfau, Rep. Prog. Phys. **72**, 126401 (2009).
[76] M. Schmitt, M. Wenzel, F. Bttcher, I. Ferrier-Barbut, and T. Pfau, Nature (London) **539**, 259 (2016).
[77] L. Chomaz, S. Baier, D. Petter, M. J. Mark, F. Wächtler, L. Santos, and F. Ferlaino, Phys. Rev. X **6**, 041039 (2016).
[78] Y. Tang, W. Kao, K.-Y. Li, S. Seo, K. Mallayya, M. Rigol, S. Gopalakrishnan, and B. L. Lev, Phys. Rev. X **8**, 021030 (2018).
[79] M. Guo, F. Bttcher, J. Hertkorn, J.-N. Schmidt, M. Wenzel, H. P. Bchler, T. Langen, and T. Pfau, Nature (London) **574**, 386 (2019).
[80] L. Tanzi, S. M. Roccuzzo, E. Lucioni, F. Fam, A. Fioretti, C. Gabbanini, G. Modugno, A. Recati, and S. Stringari, Nature (London) **574**, 382 (2019).
[81] L. Chomaz, D. Petter, P. Ilzhöfer, G. Natale, A. Trautmann, C. Politi, G. Durastante, R. M. W. van Bijnen, A. Patscheider, M. Sohmen, M. J. Mark, and F. Ferlaino, Phys. Rev. X **9**, 021012 (2019).
[82] W. Kao, K.-Y. Li, K.-Y. Lin, S. Gopalakrishnan, and B. L. Lev, Science **371**, 296 (2021).

[83] S. Baier, M. J. Mark, D. Petter, K. Aikawa, L. Chomaz, Z. Cai, M. Baranov, P. Zoller, and F. Ferlaino, Science **352**, 201 (2016).

[84] T. D. Kühner and H. Monien, Phys. Rev. B **58**, R14741 (1998).

[85] T. D. Kühner, S. R. White, and H. Monien, Phys. Rev. B **61**, 12474 (2000).

[86] S. Ejima, F. Lange, and H. Fehske, Phys. Rev. Lett. **113**, 020401 (2014).

[87] F. Grusdt, M. Höning, and M. Fleischhauer, Phys. Rev. Lett. **110**, 260405 (2013).

[88] K. Sugimoto, S. Ejima, F. Lange, and H. Fehske, Phys. Rev. A **99**, 012122 (2019).

[89] Similarly to the case of the Haldane phase, inversion symmetry is not enough to protect localized ES siDMRG calculations of Ref. [87]. However, for sufficiently strong on-site interactions, the model is effectively described by its hardcore version, where an extra chiral symmetry guarantees the presence of edge states. The regimes considered here are close to this limit.

[90] In order to select the $|L\rangle/|R\rangle$ configurations for the computation of the edge correlation length ξ_e, we fix the edge occupation by adding local chemical potentials at the edges with opposite sign.

[91] T. Kennedy and H. Tasaki, Commun. Math. Phys. **147**, 431 (1992).

[92] T. Kennedy and H. Tasaki, Phys. Rev. B **45**, 304 (1992).

[93] See Supplemental Material at http://link.aps.org/supplemental/10.1103/PhysRevLett.128.043402 which includes Refs. [94–105], for the study of the phase diagrams, the effective spin chain limit, the convergence of relevant quantities and details of the experimental realization.

[94] S. Sinha and L. Santos, Phys. Rev. Lett. **99**, 140406 (2007).

[95] F. Deuretzbacher, J. C. Cremon, and S. M. Reimann, Phys. Rev. A **81**, 063616 (2010).

[96] F. Deuretzbacher, J. C. Cremon, and S. M. Reimann, Phys. Rev. A **87**, 039903(E) (2013).

[97] N. Bartolo, D. J. Papoular, L. Barbiero, C. Menotti, and A. Recati, Phys. Rev. A **88**, 023603 (2013).

[98] C. Weitenberg, M. Endres, J. F. Sherson, M. Cheneau, P. Schauß, T. Fukuhara, I. Bloch, and S. Kuhr, Nature (London) **471**, 319 (2011).

[99] P. Würtz, T. Langen, T. Gericke, A. Koglbauer, and H. Ott, Phys. Rev. Lett. **103**, 080404 (2009).

[100] M. McDonald, J. Trisnadi, K.-X. Yao, and C. Chin, Phys. Rev. X **9**, 021001 (2019).

[101] S. Subhankar, Y. Wang, T.-C. Tsui, S. L. Rolston, and J. V. Porto, Phys. Rev. X **9**, 021002 (2019).

[102] N. Petersen, M. Trümper, and P. Windpassinger, Phys. Rev. A **101**, 042502 (2020).

[103] H. Li, J.-F. Wyart, O. Dulieu, S. Nascimbène, and M. Lepers, J. Phys. B **50**, 014005 (2017).

[104] M. Lepers (private communication).

[105] B. Huang, W. Wang, M. Bates, and X. Zhuang, Science **319**, 810 (2008).

[106] We extract $-1/\xi_e(L)$ from the slope of the linear fit $\log(|E_+ - E_-|)$ versus L, where we take values of L from the interval $[L_m - 30, L_m]$ (Fig. 1) and $[L_m - 10, L_m]$ (Fig. 2). We assume that the edge correlation length $\xi_e(L)$ is constant within the interval.

[107] X. Deng, R. Citro, E. Orignac, A. Minguzzi, and L. Santos, New J. Phys. **15**, 045023 (2013).

[108] The condition $\bar{n} = 1$ translates into $S^z_{\mathrm{tot}} = 0$ when considering spin-1 systems. By using the relation $S^z_{i,1} = 1 - n_i$, one can derive that $\Delta E_{\mathrm{charge}} = E_{\mathrm{GS}}(S^z_{\mathrm{tot}} = -1) + E_{\mathrm{GS}}(S^z_{\mathrm{tot}} = 1) - 2E_{\mathrm{GS}}(S^z_{\mathrm{tot}} = 0)$ which is the usual definition of spin gap [26].

[109] H. T. Wang, B. Li, and S. Y. Cho, Phys. Rev. B **87**, 054402 (2013).

[110] B. Yan, S. A. Moses, B. Gadway, J. P. Covey, K. R. A. Hazzard, A. M. Rey, D. S. Jin, and J. Ye, Nature (London) **501**, 521 (2013).

[111] E. Lucioni, L. Tanzi, A. Fregosi, J. Catani, S. Gozzini, M. Inguscio, A. Fioretti, C. Gabbanini, and G. Modugno, Phys. Rev. A **97**, 060701(R) (2018).

[112] J.-N. Schmidt, J. Hertkorn, M. Guo, F. Bottcher, M. Schmidt, K. Ng, S. Graham, T. Langen, M. Zwierlein, and T. Pfau, Phys. Rev. Lett. **126**, 193002 (2021).

[113] M. Lacki, M. A. Baranov, H. Pichler, and P. Zoller, Phys. Rev. Lett. **117**, 233001 (2016).

[114] M. Endres, M. Cheneau, T. Fukuhara, C. Weitenberg, P. Schauß, C. Gross, L. Mazza, M. C. Bañuls, L. Pollet, I. Bloch, and S. Kuhr, Science **334**, 200 (2011).

[115] T. A. Hilker, G. Salomon, F. Grusdt, A. Omran, M. Boll, E. Demler, I. Bloch, and C. Gross, Science **357**, 484 (2017).

[116] C. Bruder, R. Fazio, and G. Schn, Ann. Phys. (Berlin) **14**, 566 (2005).

[117] T. Giamarchi, C. Regg, and O. Tchernyshyov, Nat. Phys. **4**, 198 (2008).

[118] R. Landig, L. Hruby, N. Dogra, M. Landini, R. Mottl, T. Donner, and T. Esslinger, Nature (London) **532**, 476 (2016).

[119] S. Asban and S. Mukamel, Phys. Rev. Lett. **123**, 260502 (2019).

[120] P. Karpov and F. Piazza, arXiv:2106.13226.